PROCEEDINGS OF SPIE

SPIEDigitalLibrary.org/conference-proceedings-of-spie

Paired-agent fluorescent imaging to detect micrometastases in breast sentinel lymph node biopsy: experiment design and protocol development

Chengyue Li, Xiaochun Xu, Yusairah Basheer, Yusheng He, Husain A. Sattar, et al.

Chengyue Li, Xiaochun Xu, Yusairah Basheer, Yusheng He, Husain A. Sattar, Jovan G. Brankov, Kenneth M. Tichauer, "Paired-agent fluorescent imaging to detect micrometastases in breast sentinel lymph node biopsy: experiment design and protocol development," Proc. SPIE 10484, Advanced Biomedical and Clinical Diagnostic and Surgical Guidance Systems XVI, 1048402 (12 February 2018); doi: 10.1117/12.2290985



Event: SPIE BiOS, 2018, San Francisco, California, United States

Paired-agent fluorescent imaging to detect micrometastases in breast sentinel lymph node biopsy: experiment design and protocol development

Chengyue Li¹, Xiaochun Xu¹, Yusairah Basheer¹, Yusheng He¹, Husain A. Sattar², Jovan G. Brankov³, Kenneth M. Tichauer¹

¹Department of Biomedical Engineering, Illinois Institute of Technology, Chicago, IL 60616

²Department of Pathology, University of Chicago, Chicago, IL 60637

³Department of Electrical and Computer Engineering, Illinois Institute of Technology, Chicago, IL 60616

ABSTRACT

Sentinel lymph node status is a critical prognostic factor in breast cancer treatment and is essential to guide future adjuvant treatment. The estimation that 20-60% of micrometastases are missed by conventional pathology has created a demand for the development of more accurate approaches. Here, a paired-agent imaging approach is presented that employs a control imaging agent to allow rapid, quantitative mapping of microscopic populations of tumor cells in lymph nodes to guide pathology sectioning. To test the feasibility of this approach to identify micrometastases, healthy pig lymph nodes were stained with targeted and control imaging agent solution to evaluate the potential for the agents to diffuse into and out of intact nodes. Aby-029, an anti-EGFR affibody was labeled with IRDye 800CW (LICOR) as targeted agent and IRDye 700DX was hydrolyzed as a control agent. Lymph nodes were stained and rinsed by directly injecting the agents into the lymph nodes after immobilization in agarose gel. Subsequently, lymph nodes were frozen-sectioned and imaged under an 80-um resolution fluorescence imaging system (Pearl, LICOR) to confirm equivalence of spatial distribution of both agents in the entire node. The binding potentials were acquired by a pixel-by-pixel calculation and was found to be 0.02 ± 0.06 along the lymph node in the absence of binding. The results demonstrate this approach's potential to enhance the sensitivity of lymph node pathology by detecting fewer than 1000 cell in a whole human lymph node.

Keywords: paired-agent fluorescence imaging, micrometastses, lymph node

1. INTRODUCTION

Sentinel lymph node status is a key prognostic factor for determining the stage and guiding adjuvant treatment of breast cancer[1], as the lymphatic system is the predominant passage for tumor cell metastasis[2]. Currently, sentinel lymph node dissection is commonly performed as a standard care and followed by pathology examination to assess node metastases[3]. However, the conventional pathology laboratories only exam less than 1% of lymph node volume by sectioning lymph node as 5-µm-thick slices at 2-mm intervals and staining sections with Hematoxylin and Eosin (H&E), which provides morphological information for pathologists to identify abnormal cells. It has been demonstrated that this routine sectioning procedure might not sensitive enough to detect early stage metastatic disease, as this method was aimed to detect tumor cells deposits greater than 2 mm in diameter, defined as macrometastases[4-6]. There is some argument about the importance of detecting clusters of cells smaller than 2 mm[7]; however, there is growing evidence that patients with micrometastases (tumor clusters less than 2 mm in diameter) would benefit from more aggressive therapy. The probability of missed detection increases with decreasing size, and its estimated that 20-60% of cases with micrometastases go undetected[8].

Advanced Biomedical and Clinical Diagnostic and Surgical Guidance Systems XVI, edited by Tuan Vo-Dinh, Anita Mahadevan-Jansen, Warren S. Grundfest, Proc. of SPIE Vol. 10484, 1048402 · © 2018 SPIE · CCC code: 0277-786X/18/\$18 · doi: 10.1117/12.2290985

Numerous studies have demonstrated that micrometastases have important prognostic implication and thus enable earlier intervention for guiding therapeutic decision-making[9-11]. Many investigators have shown the increased ability to detect micrometastases in lymph node by taking extensive serial sectioning and immunohistochemistry[12-14]. However, these approaches are not cost-effective and too labor-intensive to be practical. Therefore, the demand of a diagnostic technique for breast micrometastases that will lead to more accurate detection without requiring redundant time and resources is needed.

Motivated by the drawbacks of routine histology, we developed a paired-agent imaging approach by employing a control imaging agent to allow rapid, quantitative mapping of microscopic populations of tumor cells in lymph nodes to guide pathology sectioning to reduce the false negative rate. By employing paired-agent imaging strategies, recently in a metastatic mouse model demonstrated that fewer than 200 cancer-cells can be accurately detected using a wide-field non-invasive imaging of human breast cancer spread to axillary lymph nodes[15]. This proceeding was to demonstrate the effective protocol for staining *ex vivo* lymph node and tumor 3D spheroid implantation in lymph node for further investigate the potential of paired-agent fluorescence imaging to detect micrometastases in breast sentinel lymph node biopsy.

2. METHODS AND RESULTS

2.1 Injected diffuse lymph node staining and rinsing protocol

To test the feasibility of the ratiometric paired-agent imaging method to estimate the binding potential of cancer cells, healthy pig lymph nodes were chosen based on its similarity towards the size of human lymph node. A targeted and control imaging solution was used to evaluate the potential for the agents to diffuse into and out of intact nodes. Aby-029, a clinically relevant anti-EGFR affibody, was labeled with a near-infrared fluorophore, IRDye-800CW (LICOR Biosciences) as targeted imaging agent and hydrolyzed IRDye-700DX (LICOR Biosciences), was used as control agent. Spatial distributions of both imaging agents in the entire node were compared to confirm their equivalent diffusion kinetics.

Lymph nodes were isolated from pig chins which were obtained from local butcher shop (Chicago, IL) on the day of experiment. Lymph nodes were embedded in 3% weight per volume agarose gel, needle puncture through the embedded lymph node in its greatest dimension was performed to create a simple linear channel. 27-gauge syringeneedle (BD PrecisionGlide Needle) were used in order to minimize destruction of lymph nodes. Needle was then withdrawn to the edge of the lymph node prior to staining process. Subsequently, a 500-µL volume of two imaging agents mixture were then co-injected deliberately into the lymph node through the channel, followed by 200 µL phosphate-buffered saline (PBS) injected for rinsing. Caution had to be taken during injection to ensure low pressure diffusion within the lymph node. Nodes then will be frozen and serial sectioned on a cryostat microtome at 80-µm intervals. Slides will be imaged under an 85-um resolution wide field fluorescence imaging system (LICOR) to evaluate the kinetic dynamics of the staining process.

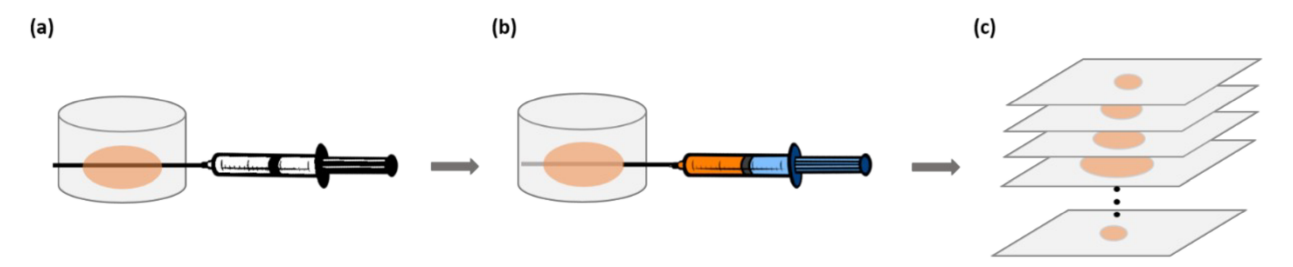


Figure 1. Stepwise illustration of injected diffuse lymph node staining and rinsing procedure. (a) Embedded lymph node was punctured though by 27-gauge syringe-needle to create a linear channel. (b) Needle was withdrawn and followed by injecting 500-μL cocktail imaging agents for staining and 200 μL for rinsing, respectively. (c) Lymph nodes serial frozen-sectioned were performed at 80-μm intervals and spatial distribution of lymph node were investigated by cross-sectional fluorescence image.

2.2 Paired-agent kinetic model

The ratiometric paired-agent imaging estimate of targeted biomolecule concentration ("Binding Potential")[16] by employing a control imaging-agent that can essentially provides a means of correcting for the influence of tissue perfusion and non-specific uptake and retention on targeted imaging agent concentrations[17, 18]. This approach assumes that the signal from the targeted imaging agent arises from concentration of imaging agent that is either bound to the specific receptor (C_b) or freely associated in the tissue (C_f) . By making the assumption that the control imaging agent signal approximates the free concentration of the targeted imaging agent, the following expression can be derived:

$$\frac{Targeted-Control}{Control} \cong \frac{C_f + C_b - C_f}{C_f} = \frac{C_b}{C_f} = K_A B \equiv Binding \ Potential \ \ (\text{BP}) \ ,$$

where K_A is the affinity of the targeted imaging agent (a constant under most conditions) and B represents the concentration of targeted biomolecules, which for cancer-specific molecules is proportional to the number cancer cells.

For the ratiometric paired-agent imaging method to accurately estimate the binding potential or concentration of cancer cells in lymph node staining applications, both the targeted and control agents must diffuse equally to all regions of the node when the node is immersed in the solution of targeted imaging agent(s) and control imaging agent mixture in the absence of cancer cells in lymph nodes.

2.3 Paired-agent imaging

Pig lymph nodes (n=5) with average size 13.02 × 9.09 mm (length × width) were stained and rinsed according to the protocol mentioned in 2.1. Subsequently, lymph nodes were frozen-sectioned at 80-μm intervals and imaged under an 85-μm resolution fluorescence imaging system (LICOR). Fluorescence at 700-740 nm and 800-840 nm (from 685 and 785 nm excitation, respectively) were acquired to evaluate similarity of uptake and washout of both targeted and control imaging agents after the process. **Fig.2a & b** display the cross-sectional lymph node of the uptake of control imaging agent (Hydrolyzed IR700DX, shown in red) and the uptake of targeted imaging agent (IR800CW labelled ABY-029 affibody, shown in green), respectively. These figures demonstrated that with the injected diffusion staining and rinsing approach, both imaging agents are capable of penetrating the entire lymph node. Binding potentials were then calculated as mentioned above on a pixel-by-pixel basis shown in **Fig. 3c**. The result demonstrated that the binding potential of targeted agent was found to be 0.02±0.06 along the lymph node in the absence of binding. These results confirmed the equivalence of spatial distribution of both agents in the entire node, and suggests that fewer than 1000 cells may be potentially observable in a whole human lymph node.

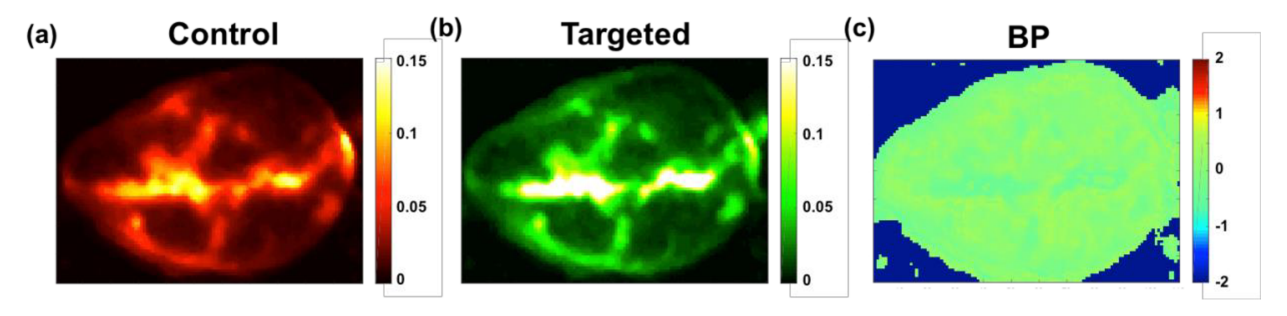


Figure 2. Images of cross-sectional pig lymph node after injected diffuse staining. The images shown in (a) and (b) are the uptake of both imaging agents in the entire lymph node. Fluorescence signals were acquired at 700 nm channel (false-colored red)

indicating hydrolyzed IR700DX, and at 800 nm channel (false-colored green) indicating IR800CW labelled ABY-029 affibody. The binding potential map of entire lymph node on a pixel-by-pixel basis are presented in (c) in the absence of binding.

2.4 GFP transfection

To further investigate the ability to detect micrometastases by using paired-agent fluorescence imaging approach, human breast cancer cell line MDA-MB-231 (ATCC, Manassas, VA) was stably transfected with GFP plasmid DNA (pAcGFP-N1, Clontech, CA) to allow validation of cancer cells. MDA-MB-231 were primarily cultured in Dulbecco's modified Eagle medium (DMEM, Corning, Manassas, VA), 10% fetal bovine serum (FBS, HyClone, Logan, Utah), 100 units/mL penicillin, and 0.1mg/mL streptomycin at 37°C in a humidified atmosphere of 5% CO₂ in air. The frozen cells were thawed and passage three generation before transfection to promote good proliferation and cell physiology.

Stable transfection was performed by Lipofectamine 3000 (Invitrogen, Grand Island, NY) according to manufacturer instruction. 1×10^6 cells were plated onto a 6-well plate one day prior transfection so that cells will be 80-90% confluent at the time of transfection, as some toxicity may be observed at lower confluency. 7.5 μ L Lipofectamine 3000 reagent, 2.5 μ g DNA and P3000 reagent were diluted separately in 125 μ L Opti-MEM reduced serum medium (Gibco, Grand Island, NY). Both of the mixtures were then combined and incubated for 10 min at room temperature. Subsequently, the DNA-lipid complex then was added to well that containing cells and medium and cells then incubated at 37°C in a CO₂ incubator. Lipofection solution was replaced by fresh medium 4 hours post-transfection.

After transfection, cells were grow and to express GFP protein for G418 resistance under non-selective condition for 72 hours. Cells were then cultured in standard medium with supplements containing 500µg/mL of G418 (Gibco) for 3 weeks for the selection of stably expressing cells. The stable transfected cells were then subjected to inspection for GFP fluorescence under a fluorescence microscope and further propagated using medium containing 250µg/mL to maintain protein selection.

2.5 Cells spheroid implantation

In order to mimic the clinical condition of cancer spread tumor draining lymph node, tumor spheroids were cultured and implanted in pig lymph nodes by direct injection. Tumor spheroids would allow cancer cells express in its original 3D architecture and offers a better control of the size of metastases in lymph nodes. In the interest of developing micrometastases model in pig lymph nodes, MDA-MB-231-GFP tumor spheroids were formed by suspending cells in culture medium containing 0.24% (w/v) methyl cellulose in round-bottom, low binding, 96 well-plates and incubated overnight at 37°C and 5% CO₂. 1×10⁴ cells were seeded in each well to achieve spheroid size of 250 µm in diameter. Tumor spheroids formation was confirmed under bright field microscope while GFP protein expression were verified under fluorescence microscope.

Considering tumor spheroid with 250 µm, diameter profile, 25-gauge syringe-needle was chosen for implantation as its inner diameter is 0.26 mm, which could prevent spheroid damage caused by needle aspiration. MDA-MB-231-GFP spheroids were implanted in 3% agarose gel to confirm spheroids were displayed as completed structures after implantation. Both bright-field and GFP-fluorescent images were acquired to observe the deposition shown in **Fig.3**. Pig lymph nodes were embedded in 3% (w/v) agarose gel prior spheroid implantation. The same technique was performed to implant tumor spheroids into pig lymph nodes. Subsequently, lymph nodes were frozen-section at 80-µm intervals and imaged under both bright-field and fluorescence microscope. Since no H&E staining has been done considering the thickness of sectioned tissue, **Fig. 3** displays no evidence of tumor spheroid deposition, however, spheroid was observed in GFP-fluorescent imaging. These images indicated that this spheroid implantation technique is effective to create a mircometastases model in pig lymph node to further investigate the paired-agent fluorescent imaging approach.

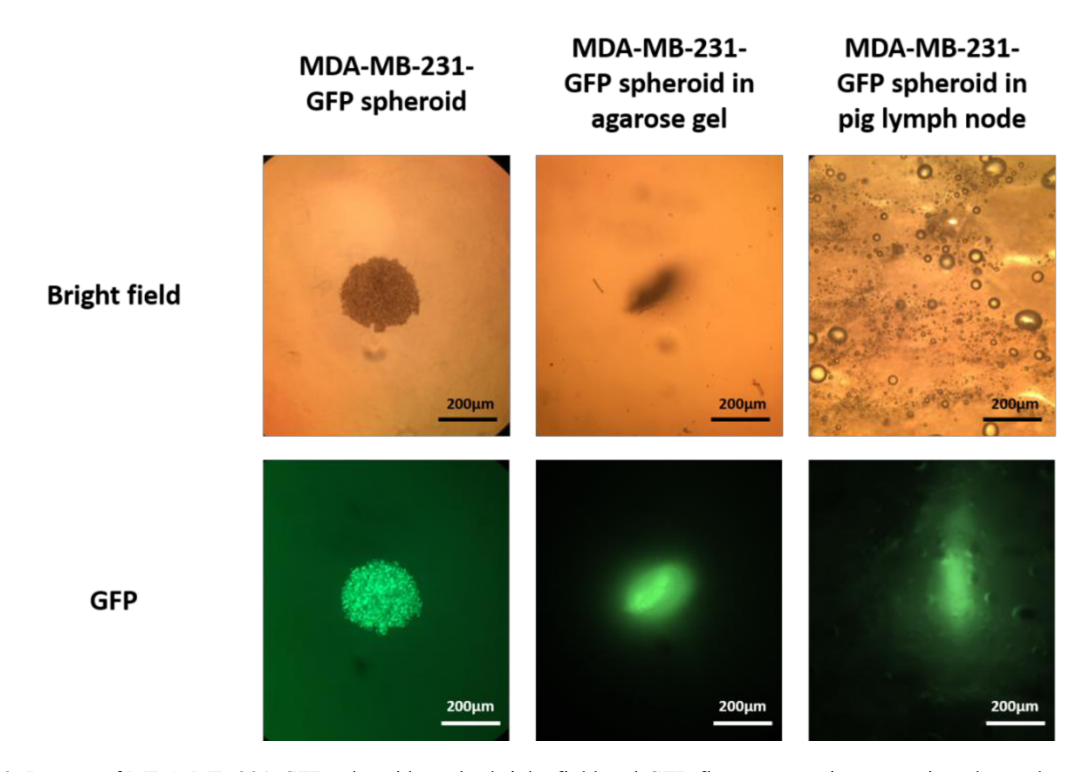


Figure 3. Images of MDA-MB-231-GFP spheroids under bright-field and GFP-fluorescent microscope in culture plate, agarose gel and pig lymph node (left to right).

3. CONCLUSIONS

With equivalent distribution of both imaging agents achieved in the entire lymph node after prolonged staining and rinsing, the results demonstrate the potential of *ex vivo* paired-agent staining and imaging of whole human lymph nodes. Average wash-in and -out rates calculated here can be used in computational models to estimate the times and doses for staining and rinsing that will optimize accuracy of the paired-agent binding potential measures, determined by simulated stain and rinse protocols that yield the lowest variance in BP estimations. With 250-µm diameter spheroid "micrometastasis" GFP transfected model being able to directly inject into a lymph node, the paired-agent fluorescence imaging and gold standard fluorescence protein microscopy would be compared to evaluate the ability to significantly improve the sensitivity of cancer cells detection for breast cancer sentinel lymph node biopsy.

REFERENCES

- [1] S. L. Chen, D. M. Iddings, R. P. Scheri *et al.*, "Lymphatic mapping and sentinel node analysis: current concepts and applications," CA Cancer J Clin, 56(5), 292-309; quiz 316-7 (2006).
- [2] M. A. Swartz, and M. Skobe, "Lymphatic function, lymphangiogenesis, and cancer metastasis," Microsc Res Tech, 55(2), 92-9 (2001).
- [3] G. H. Lyman, A. E. Giuliano, M. R. Somerfield *et al.*, "American Society of Clinical Oncology guideline recommendations for sentinel lymph node biopsy in early-stage breast cancer," J Clin Oncol, 23(30), 7703-20 (2005).

- [4] D. L. Weaver, "Pathology evaluation of sentinel lymph nodes in breast cancer: protocol recommendations and rationale," Mod Pathol, 23 Suppl 2, S26-32 (2010).
- [5] E. J. Wilkinson, L. L. Hause, R. G. Hoffman *et al.*, "Occult axillary lymph node metastases in invasive breast carcinoma: characteristics of the primary tumor and significance of the metastases," Pathol Annu, 17 Pt 2, 67-91 (1982).
- [6] N. Apostolikas, C. Petraki, and N. J. Agnantis, "The reliability of histologically negative axillary lymph nodes in breast cancer. Preliminary report," Pathol Res Pract, 184(1), 35-8 (1988).
- [7] P. P. Rosen, P. E. Saigo, D. W. Braun *et al.*, "Axillary micro- and macrometastases in breast cancer: prognostic significance of tumor size," Ann Surg, 194(5), 585-91 (1981).
- [8] K. Tew, L. Irwig, A. Matthews *et al.*, "Meta-analysis of sentinel node imprint cytology in breast cancer," Br J Surg, 92(9), 1068-80 (2005).
- [9] M. Trojani, I. de Mascarel, J. M. Coindre *et al.*, "Micrometastases to axillary lymph nodes from invasive lobular carcinoma of breast: detection by immunohistochemistry and prognostic significance," Br J Cancer, 56(6), 838-9 (1987).
- [10] "Prognostic importance of occult axillary lymph node micrometastases from breast cancers. International (Ludwig) Breast Cancer Study Group," Lancet, 335(8705), 1565-8 (1990).
- [11] P. J. Hainsworth, J. J. Tjandra, R. G. Stillwell *et al.*, "Detection and significance of occult metastases in node-negative breast cancer," Br J Surg, 80(4), 459-63 (1993).
- [12] S. Friedman, F. Bertin, H. Mouriesse *et al.*, "Importance of tumor cells in axillary node sinus margins ('clandestine' metastases) discovered by serial sectioning in operable breast carcinoma," Acta Oncol, 27(5), 483-7 (1988).
- [13] P. Ambrosch, and U. Brinck, "Detection of nodal micrometastases in head and neck cancer by serial sectioning and immunostaining," Oncology (Williston Park), 10(8), 1221-6; discussion 1226, 1229 (1996).
- [14] R. J. Cote, H. F. Peterson, B. Chaiwun *et al.*, "Role of immunohistochemical detection of lymphnode metastases in management of breast cancer. International Breast Cancer Study Group," Lancet, 354(9182), 896-900 (1999).
- [15] K. M. Tichauer, K. S. Samkoe, J. R. Gunn *et al.*, "Microscopic lymph node tumor burden quantified by macroscopic dual-tracer molecular imaging," Nat Med, 20(11), 1348-53 (2014).
- [16] M. A. Mintun, M. E. Raichle, M. R. Kilbourn *et al.*, "A quantitative model for the in vivo assessment of drug binding sites with positron emission tomography," Ann Neurol, 15(3), 217-27 (1984).
- [17] K. M. Tichauer, Y. Wang, B. W. Pogue *et al.*, "Quantitative in vivo cell-surface receptor imaging in oncology: kinetic modeling and paired-agent principles from nuclear medicine and optical imaging," Phys Med Biol, 60(14), R239-69 (2015).
- [18] K. M. Tichauer, K. S. Samkoe, W. S. Klubben *et al.*, "Advantages of a dual-tracer model over reference tissue models for binding potential measurement in tumors," Phys Med Biol, 57(20), 6647-59 (2012).